

Parametric Investigation of a 2-D Circulation Control Geometry

Thomas D. Economon

William E. Milholen II, Ph.D.

*Configuration Aerodynamics Branch
Research and Technology Directorate
Submitted: August 7, 2008*

Parametric Investigation of a 2-D Circulation Control Geometry

Thomas D. Economon
Stanford University

William E. Milholen II, Ph.D.
Configuration Aerodynamics Branch
Research and Technology Directorate
Aeronautics Research Mission Directorate

Abstract

Circulation control is an active flow control method with the potential to generate more lift than that obtained from a conventional airfoil or finite wing geometry. In general, circulation control consists of an air jet blown tangentially from a thin slot along the trailing edge of an airfoil or wing, which through the Coanda effect can be utilized for separation control or super-circulation control. The net results are a change in the circulation strength around the airfoil and, consequently, lift augmentation.

NASA considers circulation control to be a viable flow control method for lift augmentation, and subsequently has incorporated it into achieving the NASA Subsonic Fixed Wing program's Cruise Efficient Short Take Off and Landing (CESTOL) goals. The CESTOL goals have been prompted by recent airport congestion and a need for noise abatement. The implementation of circulation control as a means to improve take off and landing characteristics of aircraft could potentially provide relief on both fronts by allowing the use of under-utilized, shorter runways and by altering traffic patterns to control noise footprints.

However, as a 2004 NASA/ONR workshop revealed, performing computational fluid dynamics (CFD) on circulation control geometries has been widely unreliable. Therefore, the NASA Langley Research Center has undertaken a research program to provide CFD validation data for circulation control geometries. Starting from the unit problem and working up through full-scale complexity, the goals of the study are to provide better understanding of the complex flow physics involved and to build a database for CFD validation of circulation control cases. Through better understanding and validation, CFD would be able to provide reliable predictions and aid in the eventual implementation of full-scale circulation control.

The current project is a subset of the larger whole; this investigation dealt with a 2-D benchmark case with a simplified geometry. A parametric CFD study was performed using NASA's TetrUSS software in order to create a database for 2-D circulation control CFD validation. Several important parameters were varied and investigated such as the amount of blowing, or momentum coefficient (C_μ), the size and shape of the computational grid, and the turbulence models employed in the computations. Further, the results were compared to wind tunnel measurements of the same geometry.

The investigation yielded a set of results offering better physical understanding of the 2-D circulation control phenomenon including the effects of varying key parameters. Further, the results will act as part of a database for circulation control CFD validation and will aid in progressing the present program to more complex circulation control geometries and, ultimately, full-scale implementation.

Nomenclature

CC	circulation control
C_d	section drag coefficient
C_l	section lift coefficient
C_p	pressure coefficient
C_μ	momentum coefficient
c	chord length
h	slot exit height (0.02 in.)
L	lift
M	Mach number
NPR	nozzle pressure ratio
\dot{m}	mass flow rate
q	dynamic pressure
Re	Reynolds number
U	velocity magnitude
α	angle of attack
β	side-slip angle
ρ	density

Subscript

∞	free-stream conditions
<i>jet</i>	conditions at slot exit

Introduction

Circulation control is an active flow control method for lift augmentation which was inadvertently discovered in 1910 and has since been investigated in some form. In general, circulation control (CC) pertains to a tangentially blown jet of air from a slot along the trailing edge of an airfoil or finite wing, which through the Coanda effect can be utilized for separation control (boundary-layer control) or super-circulation control (streamline deflection caused by jet entrainment). The moniker derives from Henri Coanda who is credited with discovering the effect. While fitting his wooden aircraft wings with metal plates for the purpose of engine exhaust deflection, he unfortunately achieved quite the opposite and subsequently destroyed the aircraft.¹

The fundamental flow physics defining the CC phenomenon revolve around the introduction of energy into the flow from the pressurized slot exit and the path of this flow around the Coanda surface. After the slot exit, the wall-bounded jet entrains the outer flow, and while it has the characteristics of a boundary layer near the wall, at a distance it behaves as a free jet. The jet remains attached to the Coanda surface while the velocity is greater than that of the free stream flow due to a sub-ambient pressure and centripetal effects. As the jet velocity increases, the stagnation point translates to a more aft position on the lower side of the airfoil leading edge and the jet separation point moves clockwise around the rounded trailing edge surface as displayed in Figure

1. The amount of jet turning can be correlated to the slot exit height, jet velocity, and Coanda surface radius and geometry. Once separated, the jet penetrates the lower surface flow inducing an effective camber in the form of a pneumatic or virtual flap. An increase in jet velocity causes more entrainment and allows the separated flow to

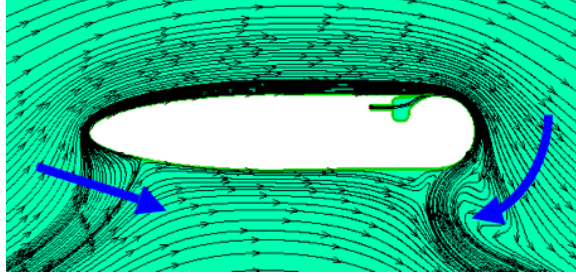


Figure 1. Typical streamline turning caused by circulation control.

penetrate the lower surface flow more deeply. The penetration, or virtual flap, results in streamline turning and, consequently, increased circulation around the airfoil.²⁻⁴ The increased circulation ultimately causes increased lift as demonstrated by their direct relationship within the Kutta-Joukowski theorem:⁵

$$L = \rho_{\infty} U_{\infty} \Gamma \quad (1)$$

As mentioned above, increasing the jet velocity results in increased entrainment and streamline turning. The non-dimensional parameter which drives this effect is the momentum coefficient, which for a 2-D application can be described by

$$C_{\mu} = \frac{\dot{m} U_{jet}}{q c} \quad (2)$$

The use of CC as a flow control method has been investigated through experiments, computations, as well as several full-scale implementations. Studies have sought to leverage the lift augmentation of CC for various reasons including low speed maneuverability,⁶ decreased landing speeds for safety considerations, lessened dependence on undamaged runways for military V/STOL operational capability,⁷ eliminating mechanical devices on wings for control or lift augmentation,⁸ decreasing take-off and landing distances, as well as aiding in aircraft noise abatement.

NASA has taken interest in CC as a flow control method for lift augmentation in order to achieve the NASA Subsonic Fixed Wing program's Cruise Efficient Short Take Off and Landing (CESTOL) goals. The CESTOL goals have been prompted by recent airport congestion and a need for noise abatement. The implementation of circulation control as a means to improve take off and landing characteristics of aircraft could potentially provide relief on both fronts by allowing the use of under-utilized, shorter runways and by altering traffic patterns to control noise footprints. Unfortunately, as revealed by a 2004 NASA/ONR workshop, CFD results on CC have been unreliable. Further, accurate results have often been based upon incorrect flow physics. The unreliability has prompted a research program at the NASA Langley

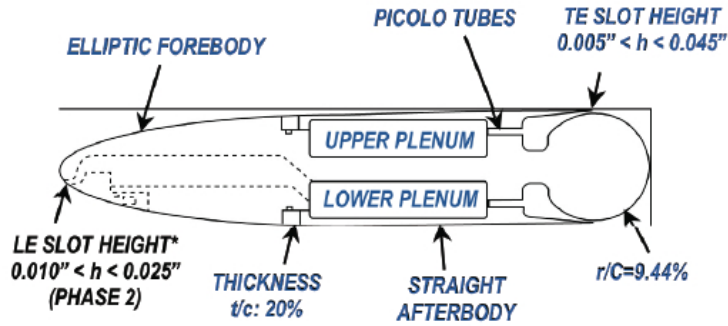


Figure 2. NASA/GTRI 2-D CFD Validation Model (CC-E0020EJ Airfoil).⁹

Research Center for the validation of CFD for CC. Starting from the unit problem and working up through full-scale complexity, the goals of the study are to provide better understanding of the complex flow physics involved and to build a database for CFD validation of CC cases. Through better understanding and validation, CFD would be able to provide reliable measurements and aid in the eventual implementation of full-scale circulation control.⁹

The following paper describes the creation of a subset of the database, namely that of a 2-D geometry benchmark case shown in Figure 2. The geometry, experimentally tested jointly in the Basic Aerodynamic Research Tunnel (BART) at NASA Langley as well as the Model Test Facility (MTF) at the Georgia Tech Research Facility, was designed to simplify the collection of quality data needed for CFD validation. The leading edge of the airfoil is elliptic in shape, while the trailing edge consists of a large circular radius allowing for accurate measurements of jet separation. The chord length is 8.6 in., and only the upper, trailing edge plenum was used for blowing with a slot exit height of 0.02 in. In the present study, a parametric CFD investigation was performed on the same geometry. Using NASA's TetrUSS software, several key parameters were varied to find the effects, including the momentum coefficient, grid size, and turbulence model used. The results of the parametric study were also compared to experimentally collected data. The three primary goals of the investigation were as follows:

- Extend the general knowledge and understanding of the complex flow physics involved in the circulation control phenomenon.
- Investigate the effects of varying key parameters and validate the effectiveness of existing CFD methods and models for circulation control geometries.
- Build portions of a database for circulation control CFD validation which will aid in the progression of complexity up to full-scale circulation control implementation.

Numerical Approach

Computations were performed using NASA’s TetrUSS (Tetrahedral Unstructured Software System) on a local computer cluster at the NASA Langley Research Center. TetrUSS is a robust CFD software package capable of rapid grid generation, inviscid and viscous flow analysis and design, as well as the employment of special boundary conditions. The software components include *GridTool* for geometry setup, *VGRID* for grid generation, and the flow solver *USM3D*. In the present study, a special procedure was utilized to create a quasi-2-dimensional, unstructured grid for the geometry of interest shown in Figure 3.

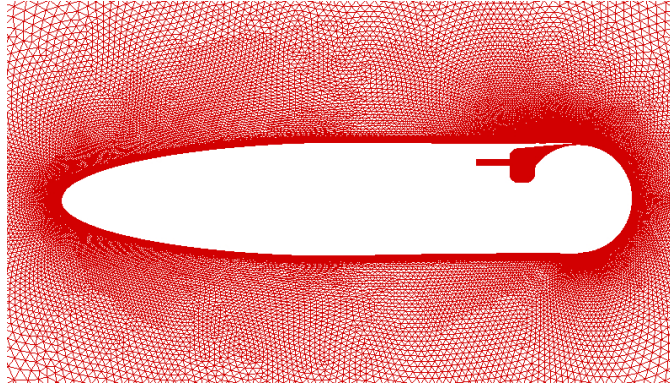


Figure 3. Quasi-2-dimensional unstructured grid.

All cases were performed as steady-state and fully turbulent. Boundary conditions were held constant for the inflow, outflow, and solid surface boundaries. In order to achieve blowing from the trailing edge slot, an engine-exhaust jet core boundary condition was applied on the left wall of the interior plenum. The amount of blowing was controlled by varying the jet stagnation pressure in relation to a constant jet static pressure. This ratio, defined as the nozzle pressure ratio (NPR), was utilized throughout the study as a direct way to control the blowing intensity. NPR is also a more readily measured quantity than C_μ in an experimental setting, which allowed for simple and consistent comparisons. Many of the flow conditions were held constant for each case. The mach number, M , remained constant at 0.1 with a Re of 5.74×10^4 . Likewise, both α and β were set to zero. Aside from when explicitly noted otherwise, $k - \epsilon$ was the employed turbulence model.

The method for parameter variation involved leaving all conditions constant apart from the variable of interest for a set of CFD computations. First, the NPR was swept across a range of typical blowing intensities used in CC. The computational mesh was then adjusted to investigate grid sensitivity effects while utilizing a single representative NPR value of 1.4. Similarly, three different turbulence models were studied: the two-equation $k - \epsilon$ model, the one-equation Spalart-Allmaras (SA) model, and the two-equation shear-stress transport (SST) model of Menter.¹⁰

Results

The following sections contain the results from the three components of the parametric investigation in the order in which they were completed. Each section contains quantitative results, figures which include comparisons to experimental data, as well as qualitative observations where applicable.

Momentum Coefficient Effects

The first parameter investigated was the momentum coefficient, or blowing intensity. Using a baseline grid and the $k - \epsilon$ turbulence model, a sweep was performed where the blowing condition was varied from an NPR of 1.05 up to 1.60 while holding all other boundary conditions and variables constant. These values correspond to C_μ values between approximately 0.03 and 0.30. The lift and drag results are presented in Figure 4. Lift and drag are of primary importance due to the high-lift goals of

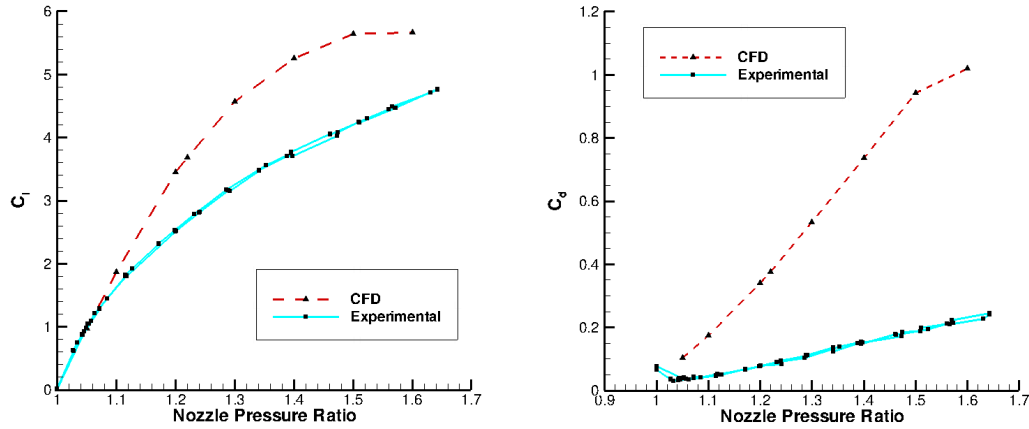


Figure 4. Effect of NPR on C_l (left) and C_d (right). ($M = 0.1$, $Re = 5.74 \times 10^4$)

CC. Substantially large lift values and relatively low drag are required in order for the technology to become advantageous. C_l values obtained from the computations increased in a near-parabola trend to a maximum of approximately 5.7. C_d values varied almost linearly with NPR to a maximum of 1. An increase in blowing intensity created a substantial rise in both lift and drag. Over the entire range, a 52% increase in NPR resulted in lift and drag coefficients growing by factors of 4.7 and 9, respectively. In general, the computational results followed the expected trend of increased lift and drag with increased blowing.

However, when comparing the CFD computations to the acquired experimental data, also shown in Figure 4, large disparities were apparent. Wind tunnel measurements found that the maximum lift and drag coefficient values for the geometry were 4.77 and 0.24, respectively. Further, the slopes of increase with NPR were lower. While the CFD and experimental results for drag do not agree at any location, the

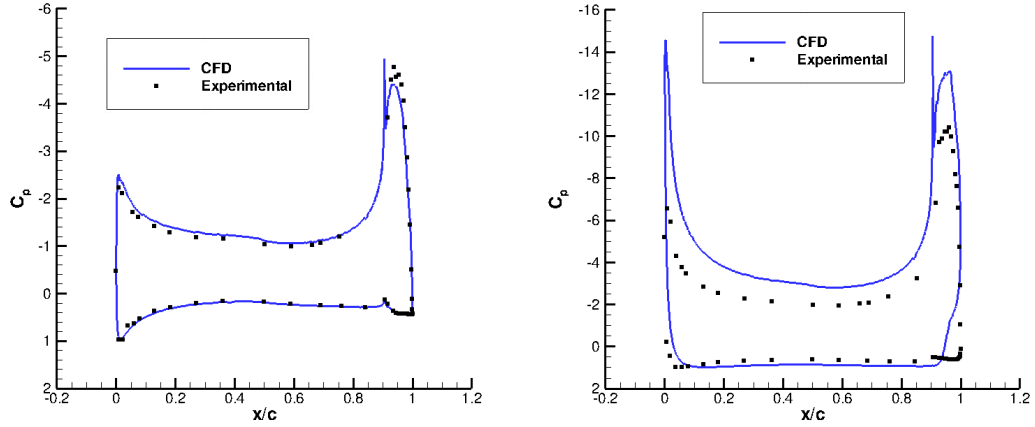


Figure 5. C_p comparisons for NPR = 1.1 (left) and NPR = 1.4 (right). ($M = 0.1$, $Re = 5.74 \times 10^4$)

lift data agree at NPR values lower than 1.10, or for C_μ values between approximately 0.03 and 0.07.

Surface C_p distributions around the airfoil geometry were examined at a low and high NPR value in order to gain insight into the disparity in lift (Figure 5). It is worth noting that the spikes seen in the CFD predictions near the trailing edge are artifacts of the jet pressure at the slot exit. For NPR = 1.1, the CFD and experimental C_p data agree well, including very detailed agreement along the lower, trailing edge near the separation point. A minor disagreement occurs along the upper, trailing edge surface where the experimental data exhibit slightly more suction. However, at an NPR value of 1.4, poor agreement was observed. Not only did the computational results largely over-predict the C_p magnitudes along the upper surface, but very poor agreement was seen on the lower surface near the trailing edge. The large over-prediction in suction surface C_p magnitudes as well as the large amount of suction near the trailing edge offered partial explanations for the variance between the CFD and experimental lift and drag results, respectively, at higher NPR values.

Mesh Refinement Effects

In order to gauge the sensitivity of the geometry and conditions to the grid shape and size, several mesh refinements were completed. The baseline unstructured grid (original) consisted of nearly 3.0×10^5 cells configured in a thin, quasi-2-dimensional manner as previously displayed in Figure 3. Due to the importance of the jet in regard to the flow physics of CC, the first investigation into the effects of mesh refinement involved both increasing the number of cells and smoothing the cell structure in and around the jet slot exit. Using the original grid as a starting point, the sourcing was modified within *GridTool* to create the finer mesh in Figure 6.

After modifying the mesh region near the slot exit, the grid consisted of approx-

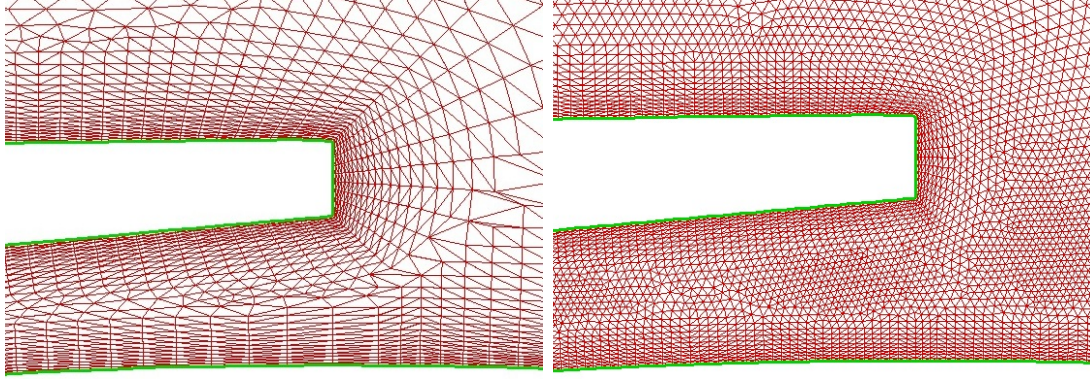


Figure 6. Grid refinement from the original (left) to the medium (right) mesh.

imately 3.14×10^5 cells, or a 5.1% increase in size. To further the mesh investigation, the newly refined mesh (medium) was scaled to be both larger (fine) and smaller (coarse) in cell number without any specific shape changes. The four different grids were each employed in cases with identical conditions, including an NPR value of 1.4, and the lift and drag results are organized in Table 1. The modification from the original grid to the medium grid yielded a 2.4% increase in the C_d , while the C_l was effectively unchanged. Changing the size of the grid from medium to coarse offered a 2.3% decrease in lift and a 1.5% increase in drag. Conversely, modifying the grid from medium to fine resulted in a lift increase of 2.5% and a drag decrease of 1.3%. The lift and drag trends for the grid sizes investigated were both nearly linear, with lift having a direct relationship to grid size and drag decreasing with more cells.

Table 1. Mesh refinement effects.

Grid	Cells	C_l	C_d
Original	298860	5.25	0.735
Coarse	164814	5.13	0.764
Medium	314211	5.25	0.753
Fine	537510	5.38	0.743

While not exorbitant, changes on the order of 1-2% are substantial when dealing with grid sensitivity. The results warrant further investigation into mesh size and shape for this CC geometry. Grid sourcing techniques should also be considered, as local alterations near the slot exit alone created noticeable changes in drag. Figure 7 presents the C_p data for each of the grid sizes studied along with the experimental data for the NPR = 1.4 condition. Only slight differences can be noticed between the original grid and the modified grids. Subsequently, all computational grids disagree with the experimental data as discussed with Figure 5. The visible differences between the grids near the trailing edge may provide evidence for the variance in lift and drag results. Although the discrepancies are minor, they emphasize the importance of

both the trailing edge region in computations and correctly modeling the separation location.

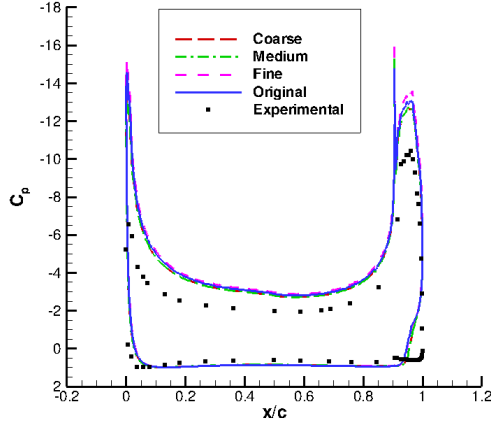


Figure 7. C_p distributions for various mesh sizes. ($M = 0.1$, $Re = 5.74 \times 10^4$, $NPR = 1.4$)

Turbulence Model Effects

The third parameter examined was the effect of turbulence models on the computational results. The fine grid was utilized for this study, along with the same $NPR = 1.4$ condition as before. Three separate turbulence models within the *USM3D* flow solver were employed within identical conditions: the two-equation $k - \epsilon$ model, the one-equation Spalart-Allmaras (SA) model, and the two-equation shear-stress transport (SST) model of Menter. Table 2 contains the lift and drag results for the three separate cases.

Table 2. Turbulence model effects for $NPR = 1.4$.

Model	C_l	C_d
$k - \epsilon$	5.38	0.743
SA	6.22	0.739
SST	5.74	0.761

In contrast to the grid sensitivity study, the turbulence models each exhibited unique and significantly different results. The lift experienced an increase of 6.7% when changing from the $k - \epsilon$ model to the SST model and a 15.6% increase to the SA model. Drag did not logically follow a trend, as the SA model demonstrated both the highest lift and lowest drag values.

The C_p distributions in Figure 8 display more disagreement among the turbulence models in comparison to the variance among grid sizes. Again, the magnitudes along

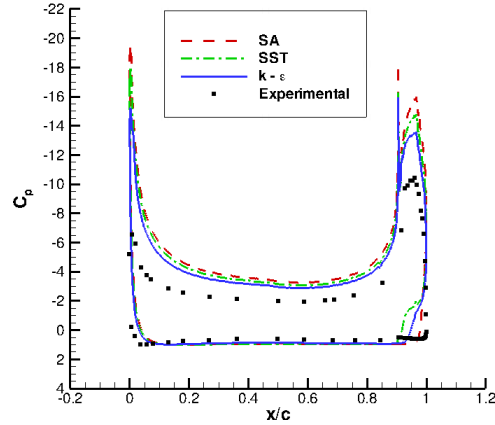


Figure 8. C_p distributions for three turbulence models. ($M = 0.1$, $Re = 5.74 \times 10^4$, $NPR = 1.4$)

the suction surface are largely over-predicted when compared to the experimental data. As priorly discussed in terms of the mesh effects, the differing results from the turbulence models further emphasize the importance of accuracy in the trailing edge region. Of particular note is the disparity between the C_p distributions on the lower, trailing edge near the separation point. The three turbulence models each provide a distinct shape in their pressure distributions, which suggested that they each modeled the separation location differently. Figure 9 depicts the separation points and streamline turning at the trailing edge of the geometry for each turbulence model. As expected, each model predicted a unique separation location, which certainly aids in explaining the differing lift and drag values between the models. By comparing the separation points in Figure 9 to the distributions in Figure 8, it is clear that the SST model over-predicts the flow turning angle and results in more suction on the lower, trailing edge surface. The $k - \epsilon$ model behaves similarly, although to a lesser extent. The SA model most closely resembles the experimental C_p data in the separation region, and thus is likely to have most accurately located the separation point. If anything, the experimental data suggests that the separation point occurs slightly higher on the trailing edge than even the SA model predicts.

To gauge the effect of the turbulence models near the airfoil surface and in the regions outside of the jet, boundary layer velocity profiles were collected along the upper surface of the airfoil at the mid-chord location, as presented in Figure 10. A glaring observation is that all three turbulence models predict much larger free-stream velocity magnitudes than the experimental data outside of the boundary layer. This is consistent with the result that all three also over-predict the lift, as larger free-stream values would seem to support more streamline turning and circulation. Similar findings at NASA Langley support the over-prediction of CC airfoil performance with CFD when compared to experimental data. CC at high lift coefficients can be difficult to predict due to wind tunnel wall effects which limit streamline turning. Similarly,

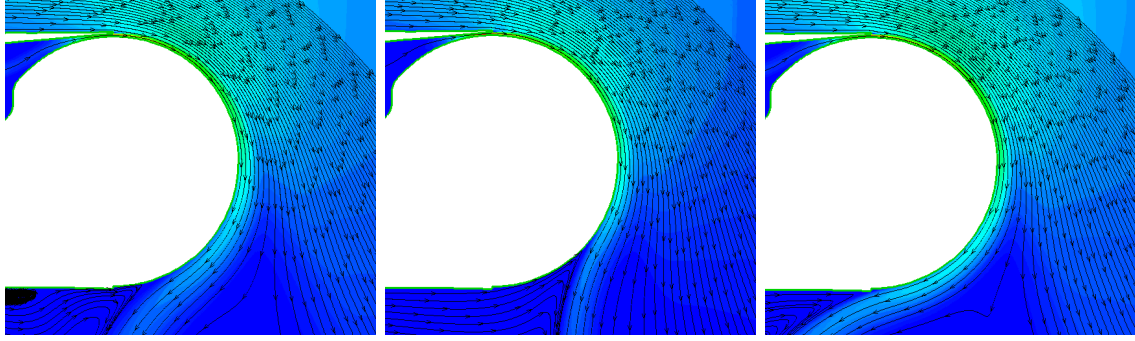


Figure 9. Separation locations for the $k-\epsilon$ (left), SA (center), and SST (right) turbulence models. ($M = 0.1$, $Re = 5.74 \times 10^4$, $NPR = 1.4$)

some discrepancy between CFD and experimental results can be attributed to the difficulty of creating a truly 2-D experiment due to 3-D effects such as juncture vortices.⁹

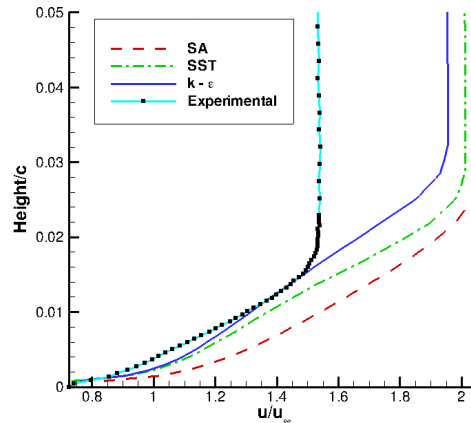


Figure 10. Effect of turbulence models on the upper surface, mid-chord boundary layer. ($M = 0.1$, $Re = 5.74 \times 10^4$, $NPR = 1.4$)

Figure 10 also details the profile shapes for each of the models. The slopes for the SA and SST models seem to more closely align with the slope of the experimental profile. By inspection, the profile shape which most closely matches the experimental data is the SA model. The large disparity in results for the various turbulence models certainly suggests that more work is required to expand the study to more grid sizes and NPR conditions. Results demonstrated here agree with other studies in that turbulence models are far from consistent in the CC environment,¹⁰ and may require special attention or modifications in order to yield more accurate and consistent results.

Conclusions

A parametric study was performed in order to better understand the flow physics involved in CC, examine the effectiveness of existing CFD techniques for use with CC geometries, as well as build portions of a database for CC CFD validation. Starting from a benchmark 2-D geometry, computational parameters were varied and their effects investigated. Namely, the effects of blowing intensity, grid sensitivity, and turbulence model sensitivity were examined.

As expected, lift and drag both increased with increased blowing intensity. However, CFD results largely over-predicted both lift and drag in comparison to experimental data. CFD predicted much larger upper surface suction and poorly modeled the trailing edge location near the jet slot exit. Mesh refinement, in terms of both sourcing modifications and cell number, caused changes on the order of 1-2% to the lift and drag results, which is considered significant when dealing with grid sensitivity. The mesh refinement results warrant further grid sensitivity studies including both examining grid sizes and sourcing techniques for CC geometries. Lastly, a turbulence model sensitivity study revealed that not only were the $k - \epsilon$, SA, and SST models inaccurate compared to the experimental data, but that they were also inconsistent when compared. Similar findings have occurred in other CC literature, suggesting that turbulence models are difficult to understand in the CC environment, and may require special attention or modifications. Further, the disagreement between CFD computations and experimental data underscored the difficulty of not only accurate modeling within the CFD environment, but also the difficulty in acquiring accurate experimental data which is free from wind tunnel and 3-D effects.

Overall, the parametric study provided a basic database for CFD validation for the 2-D CC geometry. However, the investigation also emphasized the need for more analysis and expansion into the areas discussed.

Acknowledgments

The author would like to thank NASA and the Virginia Space Grant Consortium for organizing and hosting the LARSS Program. Further thanks is certainly due to Dr. Greg Jones for access to experimental data and, most importantly, to Dr. William Milholen for his large time investment, patience, as well as excellent teaching and guidance throughout the project.

References

- ¹Wood, N. and Nielson, J., "Circulation Control Airfoils Past, Present, Future," *23rd AIAA Aerospace Sciences Meeting and Exhibit*, Reno, Nevada, January 14-17 1985.
- ²de la Montanya, J. B. and Marshall, D. D., "Circulation Control and Its Application to Extreme Short Take-Off and Landing Vehicles," *45th AIAA Aerospace Sciences Meeting and Exhibit*, Reno, Nevada, January 8-11 2007.
- ³Jones, G. S. and Englar, R. J., "Advances in Pneumatic-Controlled High-lift Systems Through Pulsed Blowing," *21st AIAA Applied Aerodynamics Conference*, Orlando, Florida, June 23-26 2003.

⁴Sellers, W. L., Jones, G. S., and Moore, M. D., "Flow Control Research at NASA Langley in Support of High-Lift Augmentation," *AIAA Biennial International Powered Lift Conference*, Williamsburg, Virginia, November 5-7 2002.

⁵Kuethe, A. M. and Chow, C.-Y., *Foundations of Aerodynamics: Bases of Aerodynamic Design*, John Wiley and Sons, Inc., 2006.

⁶Slomski, J. F., Gorski, J. J., Miller, R. W., and Marino, T., "Numerical Simulation of Circulation Control Airfoils as Affected by Different Turbulence Models," *40th AIAA Aerospace Sciences Meeting and Exhibit*, AIAA, Reno, Nevada, January 14-17 2002.

⁷Williams, S. L. and Franke, M. E., "Navier-Stokes Methods to Predict Circulation Control Airfoil Performance," *Journal of Aircraft*, Vol. 29, No. 2, March-April 1992, pp. 243-249.

⁸Englar, R. J., Smith, M. J., Kelley, S. M., and Rover, R. C., "Development of Circulation Control Technology for Application to Advanced Subsonic Transport Aircraft," *31st AIAA Aerospace Sciences Meeting and Exhibit*, Reno, Nevada, January 11-14 1993.

⁹Jones, G. S., Lin, J. C., Allan, B. G., Milholen, W. E., Rumsey, C. L., and Swanson, R. C., "Overview of CFD Validation Experiments for Circulation Control at NASA," *International Powered Lift Conference*, London, UK, July 22-24 2008.

¹⁰Swanson, R. C. and Rumsey, C. L., "Numerical Issues for Circulation Control Calculations," *3rd AIAA Flow Control Conference*, San Francisco, California, June 5-8 2006.